Available online at www.sciencedirect.com
ScienceDirect
Journal of Hazardous Materials 152 (2008) 589–600
Journal of Hazardous Materials
www.elsevier.com/locate/jhazmat

Adsorptive removal of acrylonitrile by commercial grade activated carbon: Kinetics, equilibrium and thermodynamics

Arvind Kumar, B. Prasad *, I.M. Mishra

Department of Chemical Engineering, Indian Institute of Technology Roorkee, Roorkee-247 667, Uttarakhand, India

Received 16 September 2006; received in revised form 9 July 2007; accepted 9 July 2007
Available online 21 July 2007

Abstract

The potential of activated carbons—powdered (PAC) and granular (GAC), for the adsorption of acrylonitrile (AN) at different initial AN concentrations ($50 \leq C_0 \leq 500$ mg/l) from aqueous solutions was studied over the temperature range of 303–333 K. The effect of adsorbent dosage, initial AN concentration, contact time, and the change in pH with addition of adsorbents on adsorption was studied. The Langmuir, Freundlich, Tempkin, and Redlich–Peterson (R–P) isotherm equations were used to test their fit with the experimental data, and the model parameters were determined for different temperatures. The Langmuir and R–P models were found to be the best to describe the equilibrium isotherm data of AN adsorption on PAC and GAC, respectively. Error analysis also confirmed the efficacy of the R–P isotherm to best fit the experimental data. The pseudo-second order kinetic model best represents the kinetics of the adsorption of AN onto PAC and GAC. Maximum adsorption capacity of PAC and GAC at optimum conditions of AN removal (adsorbent dose ≈ 20 g/l of solution, and equilibrium time ≈ 5 h) was found to be 51.72 and 46.63 mg/g, respectively.

Keywords: Acrylonitrile; Activated carbon; GAC; Adsorption; Kinetics; Isotherms; Error analysis; Thermodynamics

1. Introduction

Acrylonitrile (AN) (CAS no. 107-13-1) is a volatile, colourless, flammable liquid with sweet characteristic odour and is considered to be an extremely hazardous substance [1]. It is used in the production of acrylic and modacrylic fibers, resins and rubbers, and as a chemical intermediate. AN may enter the environment accidentally, during its storage and transport but the highest potential for exposure is at the work place where AN is dealt with. The chronic exposure induces several adverse effects like asphyxia, eye irritation, headache, sneezing, nausea, vomiting, weakness, lightheadedness, mild jaundice, insomnia, diarrhoea, inflammation of the respiratory tract, etc. AN affects the central and peripheral nervous system, skin, and eyes. Water improves the stability of acrylonitrile, and the technical grade product gets stabilized against self-polymerization and colour formation by the addition of hydroquinone mono methyl ether and water [2]. EPA classifies acrylonitrile as a priority pollutant, a hazardous air as well as water pollutant, and a volatile organic compound [3].

Most of the adsorption studies on the removal of toxic materials from the aqueous solutions dealt with the adsorptive equilibrium and kinetics, and used commercial grade activated carbons and low-cost adsorbents. The literature on the adsorptive removal of toxic organics and heavy metal ions is enormous. Various isotherm models, viz. two parameter models of Freundlich and Langmuir, and three parameter models of Redlich–Peterson, etc. have been used to represent the equilibrium isotherm data. The details of these models and their characteristics have been dealt with comprehensively recently by Mishra and coworkers [4–10]. Mechanistic studies to understand sorption characteristics have been reported by many investigators [4,8,10]. Most of the authors have used Vermeulen's [11] approximations to the analytical solution of a differential equation to represent the fractional approach to equilibrium and to determine the effective diffusivity of the adsorbate into the adsorbents. The effect of temperature on the adsorption phenomenon and intraparticle diffusion process has also been studied.

Except the work of Liu et al. [12] wherein the authors used natural zeolites to adsorb AN at high concentrations, no other work is available in literature dealing with the adsorp-

* Corresponding author. Tel.: +91 1332 285323; fax: +91 1332 276535.
E-mail addresses: arvinpch@yahoo.co.in (A. Kumar), bashefch@iitr.ernet.in (B. Prasad), imishfch@iitr.ernet.in (I.M. Mishra).

0304-3894/$ – see front matter © 2007 Elsevier B.V. All rights reserved.
doi:10.1016/j.jhazmat.2007.07.048

tive removal of AN from wastewaters. Activated carbons (AC)—powdered (PAC) and granular (GAC), have been used extensively for the adsorption of a variety of pollutants and toxics from aqueous solutions. The present work reports the use of PAC and GAC for the adsorptive removal of AN from aqueous solution. Effects of such parameters as adsorbent dose (m), initial AN concentration (C_0), contact time (t) and initial pH (pH_0) of the solution on the adsorption process have also been investigated. The kinetics of adsorption of AN on the adsorbents have also been studied. Equilibrium adsorption data have been fitted to various isotherm equations to determine the best isotherm model to represent the experimental sorption data.

2. Material and methods

2.1. Adsorbents and their characterization

The commercial grade PAC was obtained from HiMedia Research Laboratory, Mumbai and the GAC was obtained from S.D. Fine Chemicals, Ltd., Mumbai (India). The physicochemical characteristics of the adsorbents were determined using standard procedures. Proximate analysis was carried out using the standard procedure [13]. Bulk density was determined using MAC bulk density meter. The pore size distribution, the specific surface area and pore volume of the PAC and GAC samples were carried out at Kunash Instruments Pvt. Ltd., Mumbai, by N_2 adsorption using Micromeritics instrument (Tristar 3000) and by using Brunauer–Emmett–Teller (BET) method, using the software of Micromeritics. Nitrogen was used as cold bath (77.15 K). The Barrett–Joyner–Hanlenda (BJH) method [14] was used to calculate the mesopore distribution for the PAC and GAC. FTIR spectrometer (Thermo Nicolet, Model Magna 760) was employed to determine the presence of functional groups in all the adsorbents at room temperature. Pellet (pressed-disk) technique was used for this purpose. The pellets were prepared by mixing the adsorbent with KBr (mass ratio 100:1). The spectral range covered was from 4000 to 500 cm^{-1} scanned at the rate of 16 nm s^{-1}.

X-ray diffraction (XRD) analysis of the adsorbents was carried out using Phillips diffraction unit (Model PW1140/90), using copper as the target with nickel as the filter medium, and radiation maintained at 1.542 Å. Goniometer speed was maintained at 1° min^{-1} and the orientation was kept from 5° to 105°. A scanning electron microscope (Model SEM-501, Phillips, Holland) was used for obtaining Scanning electron microscopy (SEM) micrographs of the adsorbents

2.2. Point of zero charge (pH_{PZC})

The zero surface charge characteristics of the PAC and GAC were determined by using the solid addition method [10]. Forty millilitres of 0.1 M KNO_3 solution was transferred to a series of 100 ml stoppered conical flasks. The pH_0 values of the solutions were roughly adjusted between 2 and 12 by adding either 0.1N HCl or NaOH. The total volume of the solution in each flask was adjusted exactly to 50 ml by adding the KNO_3 solution of the same strength. The pH_0 of the solutions were then accurately noted. One gram of PAC was added to each flask, and the flask was securely capped immediately. The suspensions were then manually shaken and allowed to equilibrate for 48 h with intermittent manual shaking. The final pH values of the supernatant liquid were noted. The difference between the initial and final pH (pH_f) values ($\Delta pH = pH_0 - pH_f$) was plotted against the pH_0. The point of intersection of the resulting curve with abscissa, at which $\Delta pH = 0$, gave the pH_{PZC}. This procedure was repeated for different concentrations of KNO_3 for both the ACs. The point of zero charge for PAC is found to be as 6.5 and that for GAC to be 10.33. Fig. 1 shows the plot between ΔpH, i.e. ($pH_0 - pH_f$) and pH_0 for two ACs. This wide variation in ΔpH_{PZC} shows the difference in the surface functional groups of the ACs.

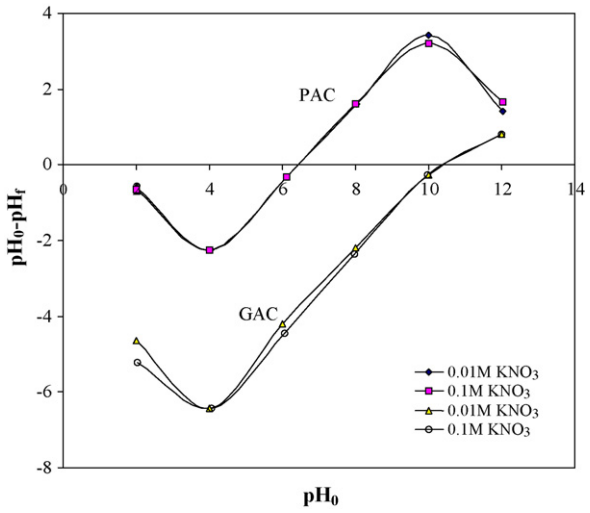

Fig. 1. Determination of the point of zero charge of PAC and GAC by the solid addition method.

2.3. Carbon pH

pH of the ACs were measured as per the standard method ASTM: D 3838-05 and their values are presented in Table 1.

2.4. Adsorbate

Laboratory grade AN, inhibited with 200 mg/l hydroquinone mono methyl ether supplied by S.D. Fine Chemicals Ltd., was used for the preparation of synthetic aqueous solutions of AN in the C_0 range of 50–500 mg/l. The required quantity of the adsorbate was accurately weighed and dissolved in a small amount of double-distilled water (DDW) and subsequently made up to one liter in a measuring flask by adding DDW. Fresh stock solution as required was prepared everyday and was kept at ambient conditions. The C_0 was ascertained before the start of each experimental run.

2.5. Analytical measurements

The concentration of AN in the aqueous solution was determined at 196 nm wavelength [15] using a high per-

Table 1
Characteristics of adsorbents

Characteristic	PAC	GAC
Proximate analysis (sample as received)		
Moisture (%)	5.65	7.70
Ash (%)	8.74	9.73
Volatile matter (%)	4.46	6.49
Fixed carbon (%)	81.12	76.08
Heating value (MJ/kg)	4.59	6.88
Bulk density (kg/m^3)	562	725
Average particle size	250 mesh	3–5 mm
Carbon pH	5.33	10.38
pH_{PZC}	6.50	10.33
Ultimate analysis (dry basis)		
C	80.25	77.16
H	1.658	5.105
N	0.158	0.025
S	0.052	0.741
Chemical analysis of ash (%)		
Insoluble matter	3.5	2.90
Silica	1.5	2.50
Ferric and alumina	3.8	3.90
CaO	84.0	84.0
Mg	2.0	2.90
Surface area (m^2/g)		
BET	798.49	870.57
Langmuir	1007.37	1015.43
t-plot micropore	804.26	965.29
t-plot external	203.12	50.14
Single point	790.06	863.19
BJH adsorption cumulative	192.63[a]	76.16[a]
Pore volume (cm^3/g)		
Single point total pore volume	0.76	0.53
t-plot micropore volume	0.25	0.33
BJH adsorption cumulative	0.30[a]	0.07[a]
Pore size (Å)		
BET adsorption average pore width	38.25	24.67
BJH adsorption average pore diameter	63.39	42.00

[a] Pores between 17 and 2000 Å.

formance liquid chromatograph (HPLC) supplied by Waters (India) Pvt. Ltd., Bangalore. Noval Pack, C_{18} column (size: 3.9 mm × 150 mm) was used in the analytical measurement of AN. Degassed organic free water was used as the solvent, keeping a flow rate of 1 ml/min as per specifications given in the user manual with the instrument. The linear portion of the calibration curve of peak area versus AN concentration was used for the determination of the unknown concentration of AN from the sample.

2.6. Batch experimental programme

For each experiment, 50 ml of AN solution of known C_0 and a known amount of the AC were taken in a 100 ml air tight glass stoppered conical flask. This mixture was agitated in a temperature-controlled shaking water bath, at a constant shaking speed. The percentage removal of AN, and the equilibrium adsorption uptake, q_e (mg/g), were calculated as:

$$\text{Percentage removal} = \frac{100(C_0 - C_e)}{C_0} \quad (1)$$

$$\text{Amount adsorbed } q_e \left(\frac{\text{mg of adsorbate}}{\text{g of adsorbent}}\right) = \frac{(C_0 - C_e)V}{w} \quad (2)$$

where C_0 is the initial sorbate concentration (mg/l), C_e the equilibrium sorbate concentration (mg/l), V the volume of the solution (ml) and w is the mass of the adsorbent (g). Control experiments were performed to check for any loss of AN from aqueous phase due to its volatilization at the headspace and its interaction with the stopper. Fifty millilitres of aqueous solution of $C_0 = 50$ and 500 mg/l were taken in two identical stoppered conical flasks and agitated in the bath at a constant shaking speed for 6 h. Thereafter, AN concentration in the aqueous phase was determined. There was no identifiable change in the AN concentration of the aqueous phase. Vidic and Suidan [16] have shown the influence of dissolved oxygen on the adsorption capacity of many organic compounds on activated carbon. However, we did not conduct any experiment for finding out the influence of dissolved oxygen. All the experiments were conducted at the maximum possible agitation speed.

3. Results and discussion

3.1. Adsorbents characterization

3.1.1. Pore characterization

The PAC pore analysis showed the dominance of micropores with pore surface area being 804 m^2/g out of the total Langmuir surface area of 1007 m^2/g. The external surface area was found to be 203 m^2/g. The BJH pore area was found to be 192 m^2/g for pore size range of 17–2000 Å. The BET average pore size was 38.3 Å where as the BJH average pore size was 63.3 Å.

The GAC analysis also showed the dominance of pore area over that of the external surface. The Langmuir surface area was found to be 1015 m^2/g with external surface area being 50 m^2/g. The BJH pore area for pore size range of 17–2000 Å was found to be 76 m^2/g. The BET average pore size was 24.6 Å, whereas the BJH average pore size was 42 Å. The analysis of both the carbons showed the predominance of microporous structure. The pore size distribution, the specific surface area and pore volume of the PAC and GAC samples are presented in Fig. 2. The details of the characteristics of PAC and GAC are given in Table 1.

3.1.2. SEM micrographs

The SEM micrographs as obtained are shown in Fig. 3 for virgin, and water- and AN-loaded PAC and GAC. It is observed that the surface texture of the adsorbents gets changed when loaded with water and AN. Both the adsorbents have random type of pores with cracks and crevices and skeletal structure at other places. Activated carbon is generally described as an amorphous form of graphite with a random structure of graphite plates having highly porous structure with a range of cracks and crevices reaching molecular dimensions.

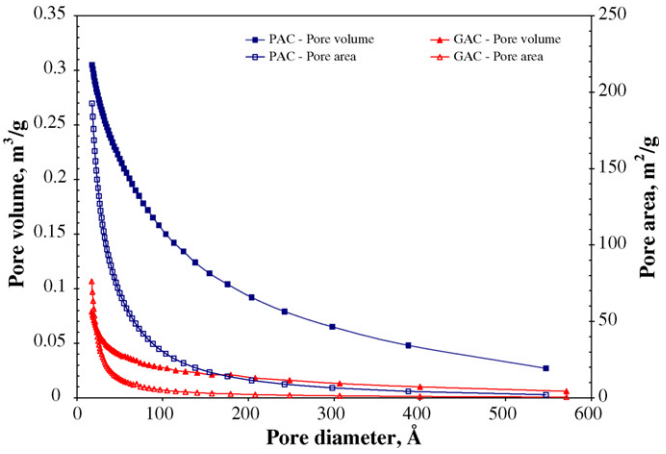

Fig. 2. Pore size distribution of PAC and GAC.

3.1.3. Thermo-gravimetric analysis

Thermal stability of PAC and GAC is directly dependent on the decomposition temperature of its various oxides and functional groups. The surface groups present on carbons and those formed as a result of interaction with oxidizing gases or solutions are generally quite stable even under vacuum at temperatures below 150 °C, irrespective of the temperature at which they were formed. However, when the carbons are heated at higher temperatures, the surface groups decompose, producing CO (150–600 °C), CO_2 (350–1000 °C), water vapour and free hydrogen (500–1000 °C) [9].

The thermo-gravimetric analysis curves (TGA, DTA and DTG) of activated carbons under inert (nitrogen) and oxidizing atmosphere at the carrier gas (nitrogen or air, as the case may be) flow rate of 400 ml/min at a heating rate of 25 K/min are shown in Fig. 4(a–d). Three different zones can be seen

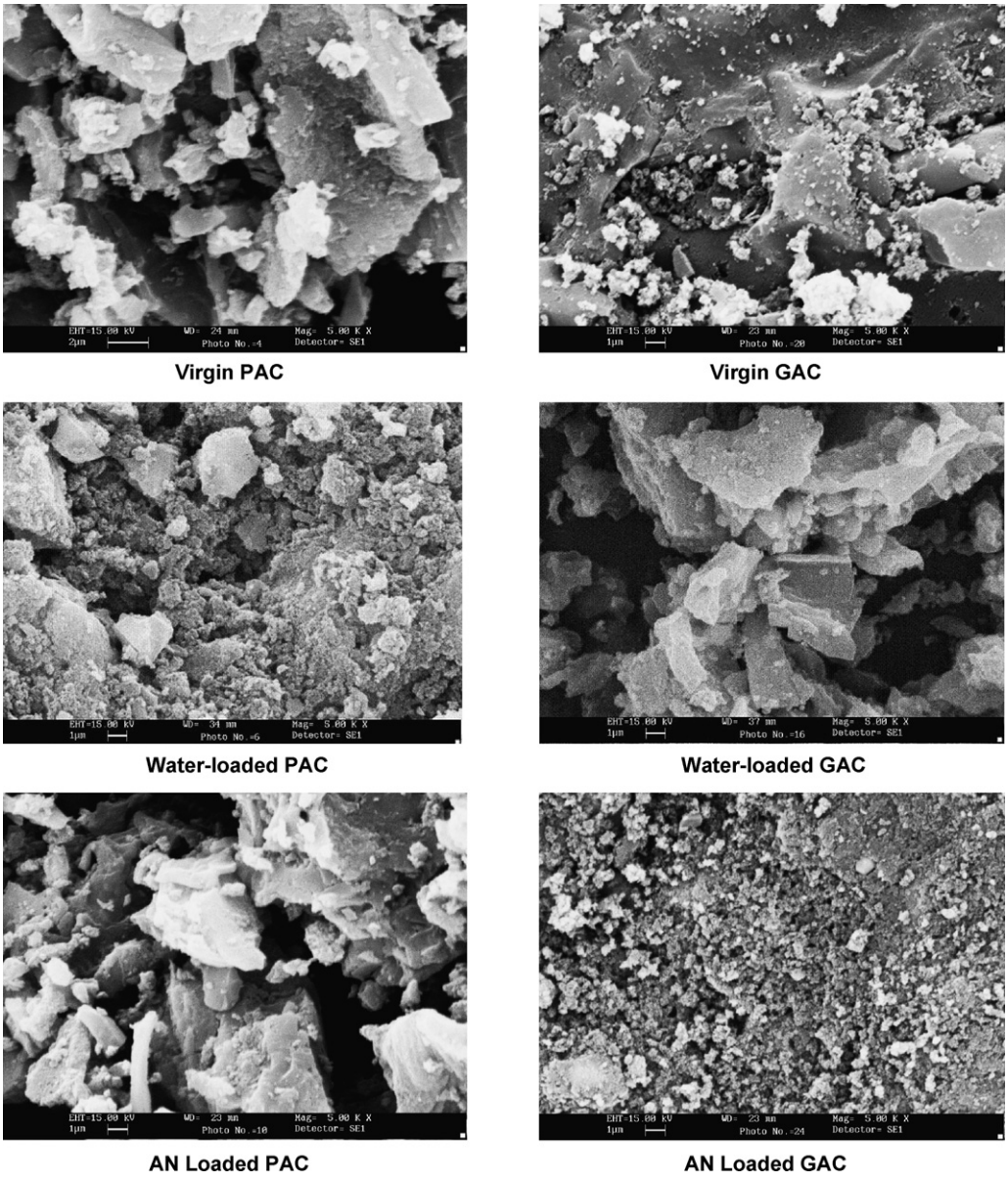

Fig. 3. SEM of virgin, water- and AN-loaded activated carbons at 5 KX.

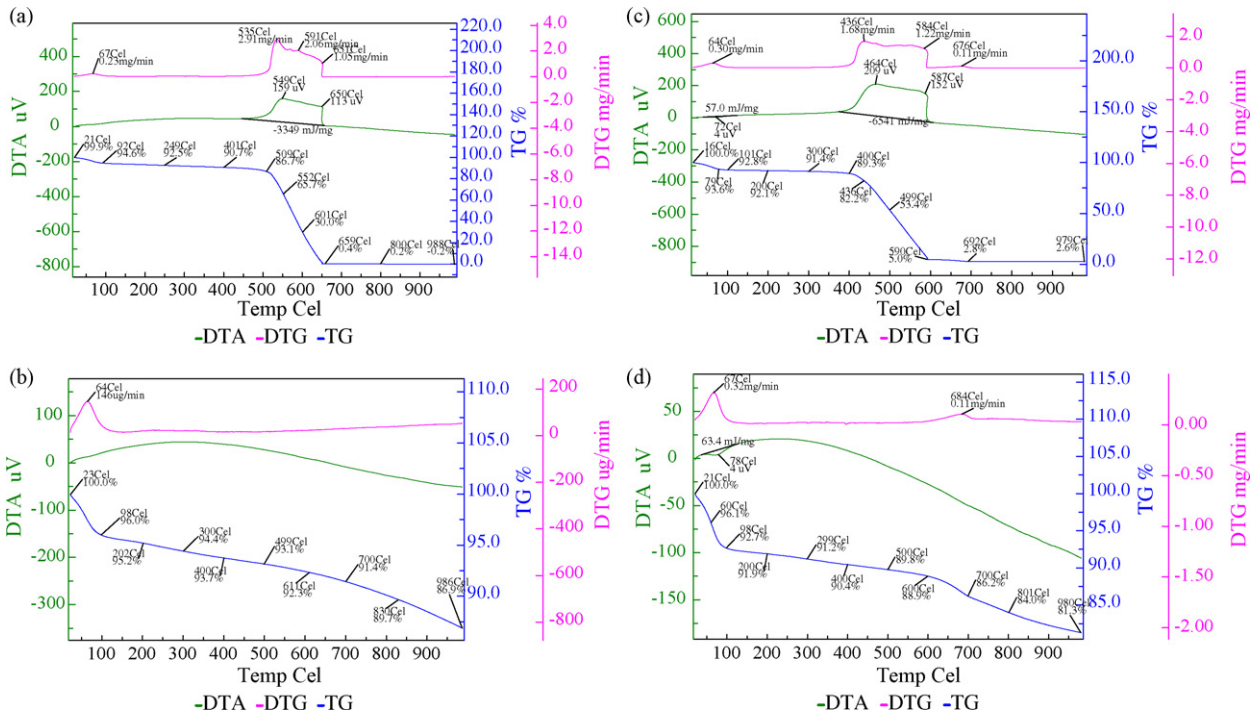

Fig. 4. (a) PAC heating rate 25 °C/min, Atm: air, flow rate: 400 ml/min. (b) PAC heating rate 25 °C/min, Atm: nitrogen, flow rate: 400 ml/min. (c) GAC heating rate 25 °C/min, Atm: air, flow rate: 400 ml/min. (d) GAC heating rate 25 °C/min, Atm: nitrogen, flow rate: 400 ml/min.

in Fig. 4(a and c) for the oxidizing atmosphere for both the carbons. For PAC (Fig. 4(a)), the first zone ranges from room temperature to 500 °C, the second zone from 500 to 650 °C, and the third zone from 650 to 1000 °C. The maximum weight loss of ~86% was recorded in the second zone, while the first zone corresponds to comparatively much smaller weight loss of ~14%. The third zone shows almost no weight loss (~0.2%) and, therefore, no degradation. For GAC under oxidizing atmosphere (Fig. 4(c)), 10.7% weight loss is observed in the first zone, from room temperature to 400 °C, ~85% weight loss in the second zone, from 400 °C to 600 °C, and a weight loss of ~2% in the third zone, from 600 to 1000 °C. Under oxidizing atmosphere, the first zone corresponds to removal of moisture and light volatiles. The active pyrolysis and oxidation zones follow this initial zone and show maximum degradation. The weight loss has been reported to be associated in part with the evolution of H_2O, CO_2 and CO. The second zone for PAC is smaller than GAC with the maximum rate of weight loss for PAC being 2.91 and 1.68 mg/min for GAC. Subsequently, the sample weight remains almost constant in the third zone with the ash remaining at 1000 °C. Thermal degradation characteristics in flowing nitrogen atmosphere show the removal of moisture of ~4 and 7.4% at a temperature of 100 °C, for PAC and GAC, respectively. Thereafter, the rate of weight loss as exemplified by the DTG curve remains almost constant up to ~500 °C (weight loss of ~3% only) for PAC and GAC (Fig. 4(b and d)). This region shows the removal of volatiles. Beyond 500 °C temperature, the rate of weight loss increases marginally with the total weight loss being ~6% for PAC. For GAC, a sudden increase in the rate of weight loss is observed at ~630 °C with the maximum rate being 0.11 mg/min at 684 °C. After 750 °C, the rate of weight loss remains constant and the maximum weight loss is found to be 8.5%. This means, that the internal structure of GAC undergoes transformations under nitrogen atmosphere with the release of decomposed matter in the gaseous form. The total weight loss of PAC and GAC under nitrogen atmosphere in the temperature range of 100–1000 °C is ~9 and 11%, respectively. The difference noticeable between the thermal degradation characteristics of PAC and GAC could be attributed to the difference in the pore size distribution of the two carbons, as their ultimate analysis gave similar results. It is seen that the average pore size of the PAC is much larger than that of GAC and hence the resistance to heat transfer and degradation will be larger for GAC than that for PAC.

3.1.4. FTIR analysis

FTIR of the virgin and loaded ACs has been carried out for both the adsorption systems, viz. AN–PAC and AN–GAC as shown in Fig. 5(a and b). The lower part of Fig. 5(a) shows the FTIR of virgin PAC and the upper part for the AN loaded PAC. The shifting of various peaks is observed. The band appearing at 3466 cm^{-1} in the spectra of virgin PAC is assigned to indicate hydrogen bonding; and at 2908 and 2843 cm^{-1} the bands are assigned to O–H stretching vibration originating in the molecule. The band appearing at 1383 cm^{-1} is assigned to symmetrical CO_2^- stretching. The bands appearing at 1247–1111 cm^{-1} are due to CH_2 deformation. In the loaded spectra of AN loaded PAC adsorption system, various new bands are seen. A new band appearing at 2347 cm^{-1} is assigned to O–H stretching for carboxylic acids. The peaks at 1630 and 1617 cm^{-1} correspond to C=C stretching. In Fig. 5(b), the lower part reflects the FTIR spectra of virgin GAC and the upper part indicates the spectra of

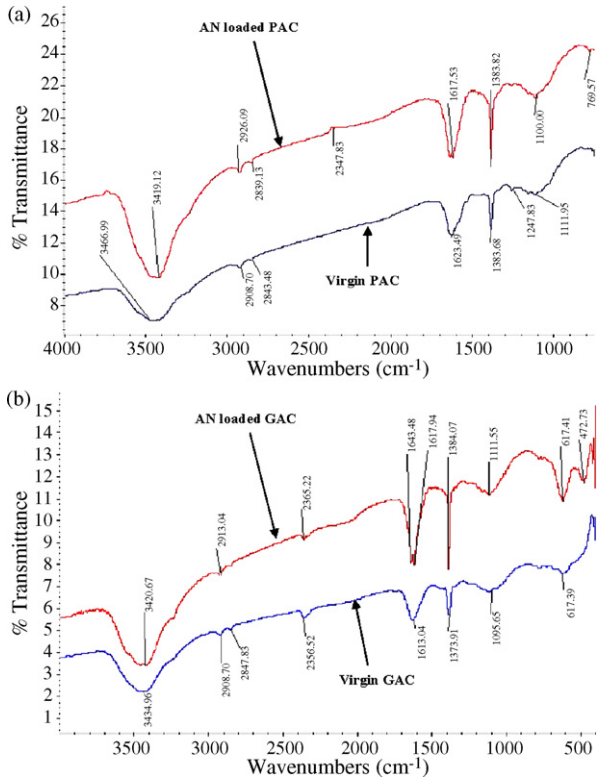

Fig. 5. (a) FTIR of virgin PAC and AN-loaded PAC. (b) FTIR of virgin GAC and AN-loaded GAC.

the AN loaded GAC. The broad band appearing at 3420 cm^{-1} is assigned to O–H hydrogen bonding. The peak at 2913 cm^{-1} shows the C–H alkanes. Peaks at 1643 and 1617 cm^{-1} show the medium bands of N–H (amines). Peak at 1384 cm^{-1} indicates symmetrical COO^- stretching. The shifting of bands occurs in AN–GAC spectra. The small band appearing at 2847 cm^{-1} represents O–H stretching. A band appearing at 2356 cm^{-1} is assigned to O–H stretching for carboxylic acids. Remaining bands in the AN–GAC spectra are almost similar to that appearing for virgin GAC.

3.1.5. XRD analysis

X-ray diffraction patterns for virgin and AN-loaded ACs are shown in Fig. 6. Minor components identified in ACs are crystalline quartz, alumina and calcium orthosilicate, whereas, wallastonite and calcium silicate and silicon oxide are the major components. Diffraction peaks corresponding to crystalline carbon were not observed in both the ACs. The broad peaks in both the samples indicate the presence of amorphous form of silica. From the SEM micrographs and X-ray diffractograms, it is seen that the activated carbons have heterogeneous surface. Proximate analysis of adsorbents showed 81.12% and 76.08% fixed carbons in PAC and GAC, respectively.

3.2. Effect of adsorbent dosage (m)

The effect of m on the uptake of AN by PAC and GAC was studied for $C_0 = 100$ mg/l. It is found that the removal of AN by PAC and GAC increases with an increase in the adsorbent dose. The removal of AN remains almost constant with a removal efficiency of ~93% for $m > 20$ g/l for PAC and the AN removal efficiency with $m > 20$ g/l of GAC is found to be ~91%. Adsorption of AN is enhanced with an increase in the adsorbent dosage up to these levels, because of availability of larger surface area and adsorption sites. At lower dosages of the adsorbents, the adsorbent surface becomes saturated with AN and a larger residual AN concentration remains in the solution. At a dosage of 20 g/l of PAC and 20 g/l GAC for $C_0 = 100$ mg/l, equilibrium conditions exist for the adsorbate–adsorbent system with almost no increase in the AN uptake by PAC and GAC. The adsorption capacity of AN on PAC and GAC is comparable. This is probably due to the same surface area of carbons. Due to the small size of AN molecule, the pore size of carbons does not significantly affect their adsorption capacity (absence of molecular sieve effect).

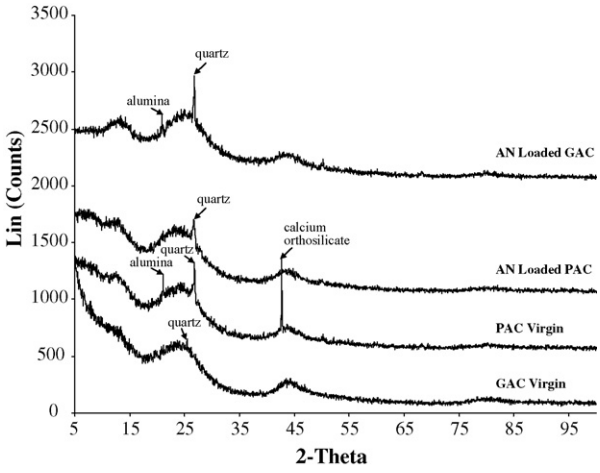

Fig. 6. XRD of virgin and AN loaded activated carbons.

3.3. Effect of contact time and initial AN concentration

The effect of contact time on the sorption uptake q_e of PAC and GAC is shown in Figs. 7 and 8, respectively. It is found that the equilibrium sorption time is very low, ~60 min for AN adsorption onto PAC, whereas, it is ~240 min for the GAC. However, the rate of AN removal is very fast by both the PAC and GAC. This is obvious from the fact that a large number of vacant surface sites are available for the adsorption during the initial stage and with the passage of time, the remaining vacant surface sites are difficult to be occupied due to repulsive forces between the solute molecules on the solid phase and in the bulk liquid phase.

Aqueous solutions of AN having $C_0 = 100$ mg/l were kept in contact with the GAC for 6 h. Since the sorption of AN remains almost constant and the variations in the adsorption uptake at 5 h and 6 h is less than 1% of that at 5 h, a steady-state approximation was assumed and quasi-equilibrium situation was assumed at $t = 5$ h. The rate of removal of AN with PAC is found to be extremely fast, with more than 91% removal obtained in 5 min. This is in contrast to the rate of removal of AN with GAC where only 46% AN removal is obtained in 5 min. The difference in

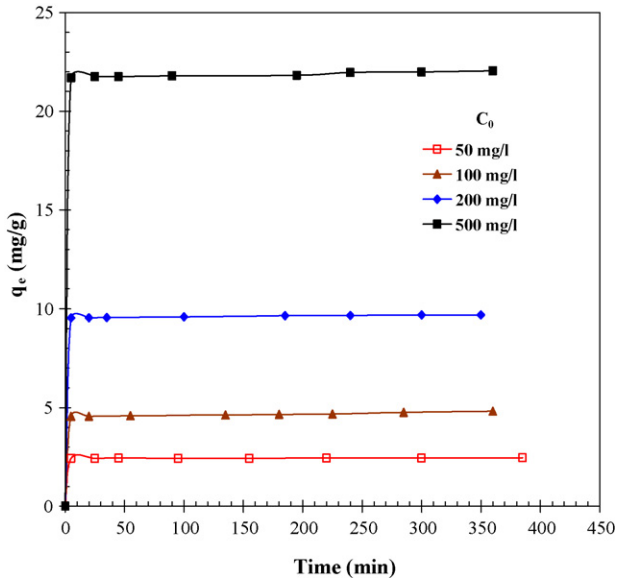

Fig. 7. Effect of initial concentration of on removal of AN–PAC adsorption system at natural pH. $T = 303$ K, $m = 20$ g/l.

adsorption rate of AN on carbons during the first 5 min could be explained. The smaller size of particles and larger pore size of PAC make it more accessible to AN by diffusion from solution than that for GAC. Significant change in residual AN concentration and q_e is observed after $t = 1$ h: 93% removal by PAC with $C_0 = 100$ mg/l and $q_e = 4.60$ mg/g, and 84% removal by GAC with $C_0 = 100$ mg/l and $q_e = 4.40$ mg/g. After 15 days treatment with both the adsorbents, the residual AN concentration in the solution is 3.59 and 4.26% for AN–PAC and AN–GAC systems, respectively. All the batch experiments were, therefore, conducted with a contact time of 2 and 5 h for AN–PAC and AN–GAC systems, respectively, under vigorous shaking conditions at natural pH for both the adsorbents.

The effect of C_0 on the extent of adsorption for AN–PAC and AN–GAC systems as a function of time are shown in Figs. 7 and 8, respectively. At any time, q_e is seen to increase with an increase of C_0. However, the adsorption rate is decreased, especially in the case of GAC, where diffusion phenomena seem to be more limiting to the adsorption rate. The C_0 provides the necessary driving force to overcome the resistance to mass transfer of AN between the aqueous phase and the solid phase. The increase in C_0 also enhances the interaction between adsorbate molecules and the vacant sorption sites on the adsorbents and the surface functional groups. Therefore, an increase in C_0 enhances the adsorption uptake of AN by PAC and GAC.

3.4. Change in pH

The solution pH_0 for $C_0 = 100$ mg/l is found to be 6.46. With the addition of both the adsorbents at $w = 20$ g/l, the solution pH changes. The pH also changes with time during the sorption process until equilibrium is attained as shown in Fig. 9. The pH change is very fast just after the addition of the adsorbents. For AN–GAC system, the pH changes from its initial value of 6.46 to about 9.71 in about 5 min and thereafter shows a very slow rise in pH with the final pH (pH_f) being 10.08 at $t = 390$ min. this is near the pH_{PZC} (10.33) of GAC. For AN–PAC system, the pH changes from its initial value of 6.46 ($\sim pH_{PZC}$ for PAC) to 8.27 in about 5 min and thereafter raises to 8.60 at $t = 200$ min and then gradually forms a plateau and stabilizes at ~pH 8.9. This again reinforces the differences in the surface functional groups of GAC and PAC and, in turn, the AN sorption efficiency of GAC and PAC. Fig. 9 supports the conclusions drawn in Section 3.3 that the sorption kinetics is very fast initially, almost instantaneous, for both the activated carbons and the sorption is seemingly absent during the later periods of contact.

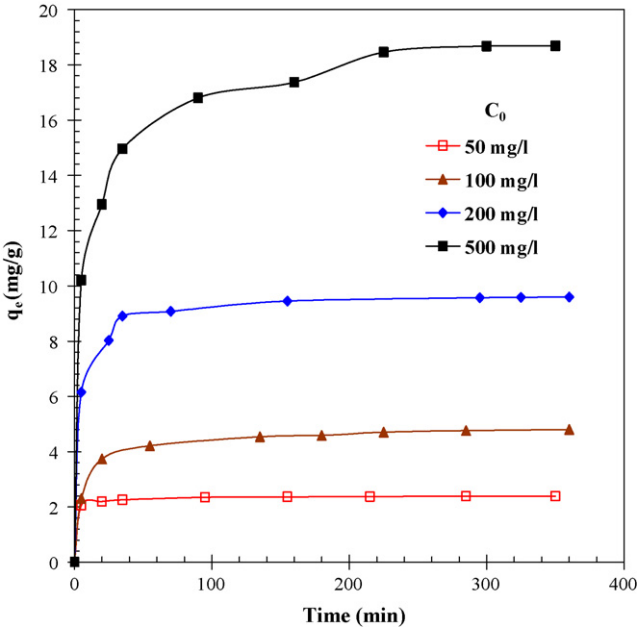

Fig. 8. Effect of initial concentration of on removal of AN–GAC adsorption system at natural pH. $T = 303$ K, $m = 20$ g/l.

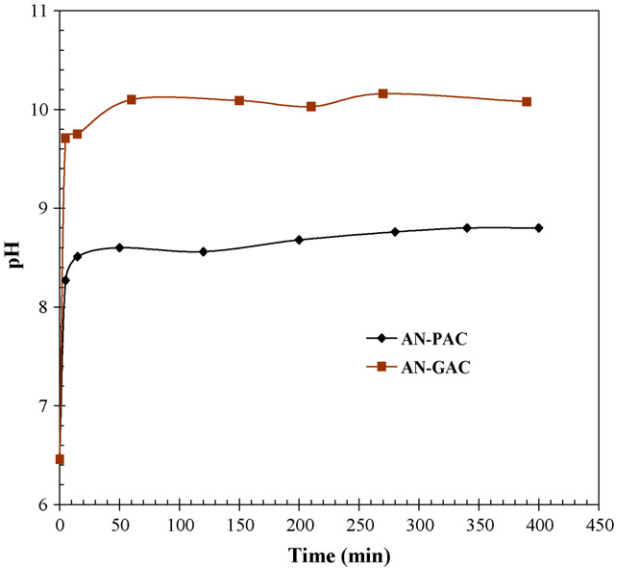

Fig. 9. pH change pattern after adding adsorbents. $T = 303$ K, $m = 20$ g/l.

3.5. Adsorption kinetics

In order to investigate the sorption kinetics of AN onto PAC and GAC, the experimental results were analyzed using pseudo-first order and pseudo-second order models [17].

3.5.1. Pseudo-first order and pseudo-second order models

The pseudo-first-order equation is given as follows [18]:

$$\frac{dq_t}{dt} = k_f(q_e - q_t) \quad (3)$$

Eq. (3) can be linearized into the following form

$$\ln(q_e - q_t) = \ln q_e - k_f t \quad (4)$$

where q_t is the amount of adsorbate adsorbed at time t (mg/g); q_e the adsorption capacity in equilibrium (mg/g), and k_f is the pseudo-first order rate constant (min^{-1}) for AN adsorption. k_f is determined from a plot of $\ln(q_e - q_t)$ versus t (not shown here). The k_f, $q_{e,exp}$ and $q_{e,cal}$ values from the pseudo-first order model are given in Table 2.

The pseudo-second order model can be represented as given below [19]:

$$\frac{dq_t}{dt} = k_s(q_e - q_t)^2 \quad (5)$$

where k_s is the pseudo-second order rate constant (g/mg min). Integrating Eq. (5) and noting that $q_t = 0$ at $t = 0$, the following equation is obtained:

$$q_t = \frac{k_s q_e^2 t}{1 + k_s q_e t} \quad (6)$$

The initial sorption rate, h (mg/g min) at $t = 0$ is defined as

$$h = k_s q_e^2 \quad (7)$$

h, q_e and k_s can be determined from the non-linear regression of Eq. (6) with the experimental data using the MicroSoft Excel spread sheet for Windows. The best-fit values of h, q_e and k_s along with the correlation coefficients for the pseudo-first order and pseudo-second order models are shown in Table 2.

The $q_{e,exp}$ and $q_{e,cal}$ values from the pseudo-second order kinetic model are very close to each other and the correlation coefficients are also found to be very high and closer to unity. Therefore, the sorption kinetics can be represented by the pseudo-second order kinetic model for the adsorption of AN onto PAC and GAC. Mall et al. [20] have reported k_s values of 0.413 and 0.069 g/mg.min for the adsorption of Congo red dye onto commercial- and laboratory-grade activated carbons. But due to different nature of the adsorbate–adsorbent systems, a direct comparison of k_s values obtained in this study with those reported in literature is not justified.

3.6. Adsorption equilibrium study

To optimize the design of an adsorption system for the adsorption of the adsorbates, it is important to establish the most appropriate correlation for the equilibrium curves. Various isotherm equations have been used to describe the equilibrium nature of adsorption. Large number of researchers in the field of environmental engineering have used Freundlich and Langmuir isotherm equations to represent equilibrium adsorption data for AC-organic contaminants systems. This, despite the fact that these equations have serious limitations on their usage. The most popular Freundlich isotherm is suitable for highly heterogeneous surfaces; however, it is valid for adsorption data over a restricted range of concentrations. For highly heterogeneous surfaces and extremely low concentrations, Henry's Law is valid. However, Freundlich equation [21] does not approach Henry's Law at vanishing concentrations. The Langmuir equation [22], although follows Henry's Law at vanishing concentrations, is valid for homogeneous surfaces. Thus, both these isotherm equations may not be suitable for AN adsorption on activated carbon for the whole range of concentrations used in the study. Temkin isotherm equation contains a factor that explicitly takes into account the interactions between adsorbing species and the adsorbate. This isotherm assumes that (i) the heat of adsorption of all the molecules in the layer decreases linearly with coverage due to adsorbate–adsorbate interactions, and (ii) adsorption is characterized by a uniform distribution of binding energies, up to some maximum binding energy [23]. The Redlich and Peterson

Table 2
Kinetic parameters for the removal of AN–PAC and AN–GAC system

Equations	AN–PAC adsorption system				AN–GAC adsorption system			
	50 mg/l	100 mg/l	200 mg/l	500 mg/l	50 mg/l	100 mg/l	200 mg/l	500 mg/l
Pseudo first order equation: $\ln(q_e - q_t) = \ln q_e - k_f t$								
k_f (min^{-1})	3.785	0.783	0.790	120.485	0.410	0.139	0.216	0.068
$q_{e,exp}$ (mg/g)	2.451	4.814	9.697	22.045	2.395	4.807	9.597	21.045
$q_{e,cal}$ (mg/g)	2.430	4.652	9.656	21.797	2.367	4.587	9.450	17.369
R^2	1.000	0.998	0.999	0.999	0.996	0.987	0.988	0.947
MPSD	0.566	3.015	1.293	1.115	4.724	10.786	9.447	28.918
Pseudo second order equation: $q_t = k_S q_e^2 t/(1 + k_S q_e t)$								
k_s (g/mg min)	32.629	1.626	1.734	333.7	0.518	0.040	0.036	0.015
h (mg/g min)	193.024	35.245	161.812	160167	2.930	0.897	3.392	4.834
$q_{e,cal}$ (mg/g)	2.432	4.655	9.659	21.797	2.370	4.723	9.635	17.650
R^2	1.000	0.998	0.999	0.999	0.998	0.998	0.997	0.966
MPSD	0.475	2.912	0.914	1.114	2.998	3.051	3.32	17.918

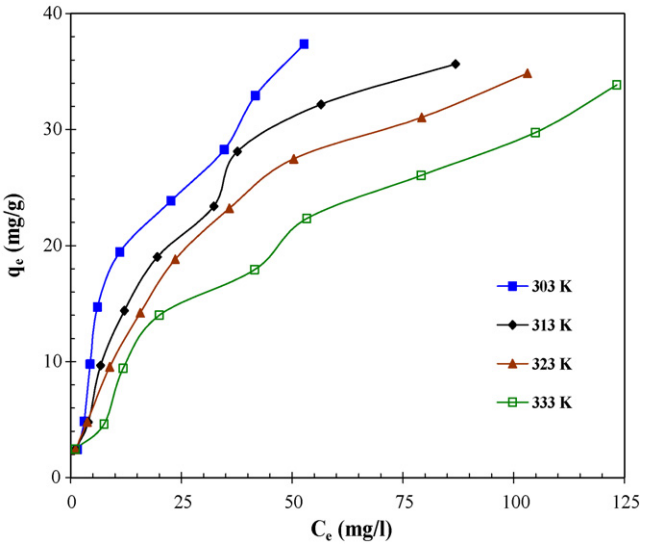

Fig. 10. Equilibrium isotherms for the adsorption of AN onto PAC at different temperatures.

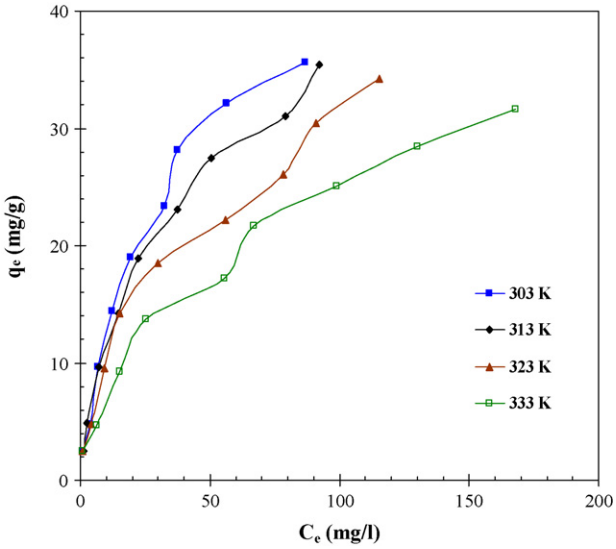

Fig. 11. Equilibrium isotherms for the adsorption of AN onto GAC at different temperatures.

(R–P) equation [24] is a three parameter-equation, often used to represent solute adsorption data on heterogeneous surfaces. This equation reduces to Freundlich equation at high concentrations and to Henry's equation at very low concentrations.

Two different error functions were also employed in this study to find out the most suitable isotherm model to represent the experimental data. The hybrid fractional error function (HYBRID) [25] and the Marquardt's percent standard deviation (MPSD) error function [26] have been used previously by a number of researchers in the field [5,6,9]. These error functions are given as

$$\text{HYBRID} = \frac{100}{n-p}\sum_{i}^{n}\left[\frac{q_{e,meas}-q_{e,calc}}{q_{e,meas}}\right]_i \quad (8)$$

Table 3
Isotherm parameters and error analysis for the removal of AN–PAC and AN–GAC system.

Constants	AN–PAC				AN–GAC			
	303 K	313 K	323 K	333 K	303 K	313 K	323 K	333 K
Langmuir isotherm: $q_e = q_m K_L C_e/(1+K_L C_e)$								
K_L (l/mg)	0.0427	0.0370	0.0353	0.0229	0.0370	0.0423	0.0345	0.0238
q_m (mg/g)	51.7210	46.6286	43.0980	42.5183	46.6288	41.5545	39.1653	37.2138
R^2	0.9810	0.9873	0.9924	0.9879	0.9873	0.9890	0.9770	0.9741
HYBRID	−0.2031	0.5774	1.3492	1.9496	0.5774	2.4043	2.9759	3.5568
MPSD	19.3395	15.3296	13.9598	27.1498	15.3297	13.6340	19.1517	25.8657
Freundlich isotherm: $q_e = K_F C_e^{1/n}$								
K_F (mg/g)/(mg/l)$^{1/n}$	2.7111	2.5053	2.4357	2.1319	2.5053	2.7483	2.4940	2.1990
$1/n$	0.6989	0.6405	0.6058	0.5734	0.6405	0.5836	0.5590	0.5266
R^2	0.9574	0.9878	0.9935	0.9846	0.9878	0.9934	0.9914	0.9934
HYBRID	−4.0352	−1.1965	−0.6181	−1.5343	−1.1965	−0.6262	−0.7669	−0.5923
MPSD	28.4812	16.0037	11.2359	19.2853	16.0037	11.4029	12.1977	11.2364
Temkin isotherm: $q_e = B_1 \ln(K_T C_e)$								
K_T (l/mg)	0.6845	0.6761	0.6519	0.5590	0.6761	0.7668	0.6787	0.5932
B_1	9.5770	8.1368	7.5169	6.7327	8.1368	7.3324	6.7654	5.9414
R^2	0.9874	0.9655	0.9674	0.9350	0.9655	0.9728	0.9593	0.9424
HYBRID	6.1072	16.0114	16.2277	13.6463	16.0114	14.7090	14.4891	13.6653
MPSD	38.6607	88.9240	80.4538	104.4845	88.9240	59.9385	78.4516	88.0334
R–P isotherm: $q_e = K_R C_e/(1+a_R C_e^{\beta})$								
K_R (l/mg)	210.8830	4.1773	4.3056	25.0326	4.1900	2.9840	5.8607	82.7253
a_R	76.9157	0.8129	0.9459	10.8317	0.8180	0.3015	1.5362	36.7582
β	0.3030	0.5077	0.5222	0.4428	0.5070	0.6957	0.5277	0.7480
R^2	0.8190	0.9703	0.9907	0.9720	0.9703	0.9992	0.9887	0.9917
HYBRID	−4.0493	−1.2544	−0.4285	−1.6874	−1.2528	−0.0835	−0.7345	−0.6189
MPSD	28.4402	14.6680	8.8838	19.7610	14.6701	2.9459	11.5099	11.3591

$$\text{MPSD} = 100\sqrt{\frac{1}{n-p}\sum_{i}^{n}\left|\frac{q_{e,meas}-q_{e,calc}}{q_{e,meas}}\right|_{t}^{2}} \quad (9)$$

HYBRID was developed to improve the fit of the square of errors function at low concentration values. The MPSD is similar in some respects to a geometric mean error distribution modified according to the number of degrees of freedom of the system.

3.6.1. Effect of temperature

Equilibrium isotherms for AN adsorption onto GAC and PAC at various temperatures are shown in Figs. 10 and 11, respectively. It is found that the adsorption of AN decreases with an increase in temperature. It can, therefore, be inferred that the adsorption is exothermic in nature. The trend obtained is in agreement with the general adsorption processes.

3.6.2. Choosing best isotherm model

Since each of the error functions produces a different set of isotherm parameters, an overall optimum parameter set is difficult to identify directly. Thus, a normalization of each parameter is employed in order to have a better comparison between the parameter sets for the single isotherm model [27]. In the normalization process, each error function was selected and the results for each parameter set were determined. Secondly, the errors determined for a given error function were divided by the maximum error to obtain the normalized errors for each parameter set. Lastly, the normalized errors for each parameter set were summed up.

Langmuir, Freundlich, Temkin, and R–P isotherm constants were determined from the plots of $1/q_e$ versus $1/C_e$; $\ln q_e$ versus $\ln C_e$, q_e versus $\ln C_e$, and $\ln(K_R C_e/q_e - 1)$ versus $\ln C_e$, respectively, at 303, 313, 323 and 333 K using MS Excel for Windows. The isotherm constants and R^2 values for all the isotherms studied are listed in Table 3.

Comparison of R^2 values for various isotherms for AN–PAC and AN–GAC systems shows that these values are closer to unity for R–P and Freundlich isotherms. By comparing the results of the values for the error function MPSD and HYBRID (Table 3), it can be concluded that the R–P and Langmuir isotherms generally best represent the equilibrium data of AN onto PAC and GAC. Comparable fit of various isotherm models for the adsorption of AN onto PAC and GAC at 313 K is shown in Figs. 12 and 13. It is seen that the Langmuir and R–P equations describe best the experimental equilibrium data.

Freundlich constants, K_F and $1/n$ indicate the adsorption capacity and adsorption intensity, respectively. Higher the value of $1/n$, the higher will be the affinity between the adsorbate and the adsorbent, and the heterogeneity of the adsorbent sites. The $1/n$ value indicates the relative distribution of energy sites and depends on the nature and strength of the adsorption process. For example, $1/n = 0.81$ refers to the fact that 81% of the active adsorption sites have equal energy level [5]. It is found from Table 3 that the PAC is more heterogeneous in nature as compared to GAC. Since $1/n < 1$, AN is favorably adsorbed by PAC and GAC at all temperatures. The surface heterogeneity is due to the existence of crystal edges, type of cations, surface charges,

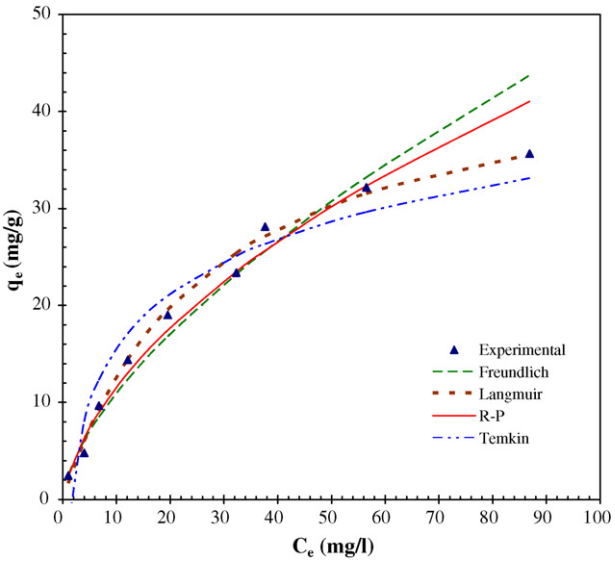

Fig. 12. Comparison of the fit of various isotherm equations for the adsorption of AN onto PAC at temperature 313 K. $t = 6$ h.

and the degree of crystallinity of the surface. The net effect of these factors is temperature dependent. The Freundlich isotherm does not predict the saturation of the adsorbent surface by the adsorbate [4]. The value of K_F can be taken as a relative indicator of the adsorption capacity of activated carbons for a narrow sub-region having equally distributed energy sites for the sorption of AN. The magnitude of K_F also showed the lower uptake of AN at higher temperatures indicating exothermic nature of adsorption process. The q_m is the monolayer saturation at equilibrium, whereas K_L corresponds to the concentration at which the amount of AN bound to the adsorbent is equal to $q_m/2$. This indicates the affinity of the AN to bind with the adsorbents. A high K_L value indicates a higher affinity. The data in Table 3 also indicate that the values of q_m and K_L decreased with an

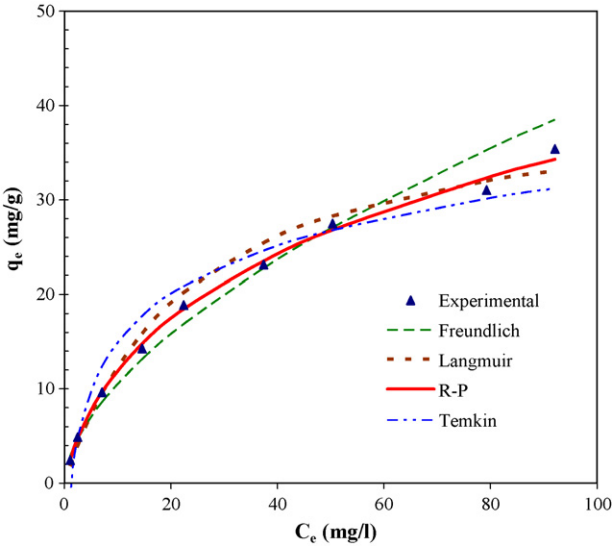

Fig. 13. Comparison of the fit of various isotherm equations for the adsorption of AN onto GAC at temperature 313 K. $t = 6$ h.

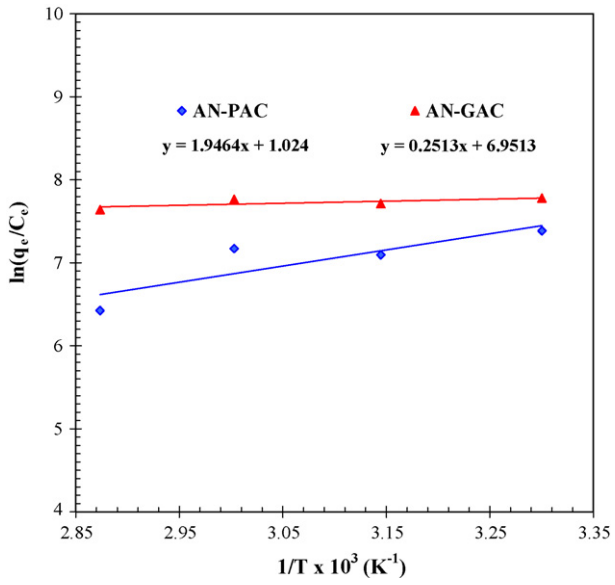

Fig. 14. The effect of temperature on the equilibrium distribution coefficient AN. Initial concentration $C_0 = 50$ mg/l, $t = 6$ h, $m = 20$ g/l.

increase in temperature confirming the exothermic nature of the overall sorption process for AN–GAC and AN–PAC systems. The fact that the adsorption capacity is increasing with a temperature decrease reveals that the diffusion process (endothermic process) does not significantly control the adsorption rate.

3.7. Adsorption thermodynamics

The temperature dependence of AN uptake was studied by performing batch experiments at 303, 313, 323 and 333 K. The standard enthalpy change was estimated by applying Van't Hoff equation:

$$\ln k_d = -\frac{\Delta H^\circ}{R}\frac{1}{T} + \frac{\Delta S^\circ}{R} \tag{10}$$

and

$$k_d = \left(\frac{C_0 - C_e}{C_e}\right)\left(\frac{V\rho}{w}\right) = \frac{q_e \rho}{C_e} \tag{11}$$

where $\rho = 1000\ \mathrm{kg/m^3}$; the density of the solution mixture, ΔH° the standard enthalpy change (J/mol), ΔS° the standard entropy change (J/mol K), T the absolute temperature (K), and k_d is the distribution coefficient. The Van't Hoff plot for AN adsorption onto GAC and PAC is shown in Fig. 14. The ΔH° and ΔS° for AN can be calculated from the slope of the straight line. The value of ΔH° for AN–PAC and AN–GAC, adsorption systems were found to be -16.18 and -2.08 kJ/mol, respectively. The values of ΔS° for the respective systems were found to be 8.51 and 57.79 kJ/mol K, respectively, indicating that the adsorption process is exothermic in nature. The positive value of ΔS° suggests an increased randomness at the solid–solution interface, and an increase in the degree of freedom of the adsorbed species.

4. Conclusion

The present study shows that the powdered- and granular-activated carbons are effective adsorbents for the removal of AN from aqueous solution. Higher percentage of AN removal by PAC and GAC was possible provided that the concentration of AN in the solution was low. Optimum PAC and GAC dosage was 20 g/l. The optimum equilibrium time for AN adsorption onto PAC and GAC was 2 and 5 h, respectively. The adsorption capacity of AN on PAC and GAC is comparable. This is probably due to the same surface area of carbons. Due to the small size of AN molecule, the pore size of carbons does not significantly affect their adsorption capacity (absence of molecular sieve effect). Adsorption kinetics was found to follow second-order rate expression. Equilibrium adsorption data for AN onto PAC and GAC were best represented by the Langmuir and R–P isotherms. Adsorption of AN is favourably influenced by a decrease in the temperature indicating exothermic nature of the adsorption process. Overall, AN is excellently adsorbed by both PAC and GAC from the aqueous solution.

References

[1] Agency for Toxic Substances and Disease Registry (ATSDR), Toxicological Profile for Acrylonitrile, U.S. Public Health Service, U.S. Department of Health and Human Services, Atlanta, GA, 1990.
[2] The Chemistry of Acrylonitrile, second ed., American Cyanamid Company, New York, 1959, 272 pp.
[3] L.H. Keith, W.A. Telliard, Priority pollutants: a perspective view, Environ. Eng. Sci. 13 (1979) 416–423.
[4] V.C. Srivastava, M.M. Swamy, I.D. Mall, B. Prasad, I.M. Mishra, Adsorptive removal of phenol by bagasse fly ash and activated carbon: equilibrium, kinetics and thermodynamics, Colloid. Surf. A 272 (2006) 89–104.
[5] V.C. Srivastava, I.D. Mall, I.M. Mishra, Equilibrium modelling of single and binary adsorption of cadmium and nickel onto bagasse fly ash, Chem. Eng. J. 117 (1) (2006) 79–91.
[6] V.C. Srivastava, I.D. Mall, I.M. Mishra, Modelling individual and competitive adsorption of cadmium(II) and zinc(II) metal ions from aqueous solution onto bagasse fly ash, Sep. Sci. Technol. 41 (2006) 2685–2710.
[7] V.C. Srivastava, I.D. Mall, I.M. Mishra, Characterization of mesoporous rice husk ash (RHA) and adsorption kinetics of metal ions from aqueous solution onto RHA, J. Hazard. Mater. 134 (2006) 257–267.
[8] M.M. Swamy, I.D. Mall, B. Prasad, I.M. Mishra, Removal of phenol by adsorption on coal fly ash and activated carbon, Pollut. Res. 16 (1997) 170–175.
[9] I.D. Mall, V.C. Srivastava, N.K. Agarwal, Removal of orange-G and methyl violet dyes by adsorption onto bagasse fly ash—kinetic study and equilibrium isotherm analyses, Dyes Pigments 69 (2006) 210–223.
[10] D.H. Lataye, I.M. Mishra, I.D. Mall, Removal of pyridine from aqueous solution by adsorption on bagasse fly ash, Ind. Eng. Chem. Res. 45 (2006) 3934–3943.
[11] T. Vermeulen, Theory for irreversible and constant pattern solid diffusion, Ind. Eng. Chem. 45 (1953) 1664–1670.
[12] Y. Liu, H. Han, X. Zhang, P. Lu, F. Zhang, Adsorption of acrylonitrile by natural zeolite, ACS Div. Environ. Chem. 43 (2) (2003) 6.
[13] IS 1350 (Part I), Methods of Test for Coal and Coke Proximate Analysis, Bureau of Indian Standards, Manak Bhawan, New Delhi, India, 1984.
[14] E.P. Barret, L.G. Joyner, P.P. Hanlenda, The determination of pore volume and area distributions in porous substances. I: Computations from nitrogen isotherms, J. Am. Chem. Soc. 73 (1951) 373–380.
[15] Acrylamide, Acrylonitrile and Acrolein by HPLC, US EPA Method 8316, Washington, DC, 1987.

[16] R.D. Vidic, M.T. Suidan, Role of dissolved oxygen on the adsorptive capacity of activated carbon for synthetic and natural organic matter, Environ. Sci. Technol. 25 (1991) 1612–1618.
[17] V.C. Srivastava, I.D. Mall, N.K. Agarwal, I.M. Mishra, Adsorptive removal of malachite green dye from aqueous solution by bagasse fly ash and activated carbon—kinetic study and equilibrium isotherm analyses, Colloid. Surf. A 260 (2005) 17–28.
[18] C.J. Rivard, K. Grohmann, Degradation of furfural (2-furaldehyde) to methane and carbon dioxide by an anaerobic consortium, Appl. Biochem. Biotech. 28/29 (1991) 285–295.
[19] Y.S. Ho, G. McKay, Pseudo-second order model for sorption processes, Process Biochem. 34 (1999) 451–465.
[20] V.C. Srivastava, I.D. Mall, N.K. Agarwal, I.M. Mishra, Removal of congo-red from aqueous solution by bagasse fly ash and activated carbon: kinetic study and equilibrium isotherm analyses, Chemosphere 61 (2005) 492–501.
[21] H.M.F. Freundlich, Over the adsorption in solution, J. Phys. Chem. 57 (1906) 385–471.
[22] I. Langmuir, The adsorption of gases on plane surfaces of glass, mica, and platinum, J. Am. Chem. Soc. 40 (1918) 1361–1403.
[23] M.J. Temkin, V. Pyzhev, Kinetics of ammonia synthesis on promoted iron catalysts, Acta Physicochim. URSS 12 (1940) 327–356.
[24] O. Redlich, D.L. Peterson, A useful adsorption isotherm, J. Phys. Chem. 63 (1959) 1024–1026.
[25] J.F. Porter, G. McKay, K.H. Choy, The prediction of sorption from a binary mixture of acidic dyes using single- and mixed-isotherm variants of the ideal adsorbed solute theory, Chem. Eng. Sci. 54 (1999) 5863–5885.
[26] D.W. Marquardt, An algorithm for least squares estimation of nonlinear parameters, J. Soc. Ind. Appl. Math. 11 (1963) 431–441.
[27] Y.C. Wong, Y.S. Szeto, W.H. Cheung, G. McKay, Adsorption of acid dyes on chitosan—equilibrium isotherm analyses, Process Biochem. 39 (2004) 693–702.